
Reprint Series
Science
21 December 2012 | $10
BREAKTHROUGH
of the YEAR
The HIGGS
BOSON
AAAS

ARTICLE

A New Boson with a Mass of 125 GeV Observed with the CMS Experiment at the Large Hadron Collider

The CMS Collaboration*†

The Higgs boson was postulated nearly five decades ago within the framework of the standard model of particle physics and has been the subject of numerous searches at accelerators around the world. Its discovery would verify the existence of a complex scalar field thought to give mass to three of the carriers of the electroweak force—the W^+, W^-, and Z^0 bosons—as well as to the fundamental quarks and leptons. The CMS Collaboration has observed, with a statistical significance of five standard deviations, a new particle produced in proton-proton collisions at the Large Hadron Collider at CERN. The evidence is strongest in the diphoton and four-lepton (electrons and/or muons) final states, which provide the best mass resolution in the CMS detector. The probability of the observed signal being due to a random fluctuation of the background is about 1 in 3×10^6. The new particle is a boson with spin not equal to 1 and has a mass of about 125 giga–electron volts. Although its measured properties are, within the uncertainties of the present data, consistent with those expected of the Higgs boson, more data are needed to elucidate the precise nature of the new particle.

The standard model (SM) of particle physics (*1*–*3*) describes the fundamental particles, quarks and leptons, and the forces that govern their interactions. Within the SM, the photon is massless, whereas the masses of the other carriers of the electroweak force, the $W^{\pm}$ and Z^0 gauge bosons, are generated through a symmetry-breaking mechanism proposed by three groups of physicists (Englert and Brout; Higgs; and Guralnik, Hagen, and Kibble) (*4*–*9*). This mechanism introduces a complex scalar field, leading to the prediction of a scalar particle: the SM Higgs boson. In contrast, all known elementary bosons are vector particles with spin 1. In the SM, the scalar field also gives mass to the fundamental fermions through a Yukawa interaction (*1*–*3*). The Higgs boson is predicted to decay almost instantly to lighter particles.

The theory does not predict a specific mass for the Higgs boson. Moreover, the properties of the Higgs boson depend strongly on its mass. General arguments indicate that its mass should be less than about 1 TeV (*10*–*13*), although searches for the SM Higgs boson conducted before those at the Large Hadron Collider (LHC) have excluded the mass region below 114.4 GeV (*14*). Searches at the Tevatron have excluded a narrow mass region near 160 GeV (*15*) and recently reported an excess of events in the range from 120 to 135 GeV (*16*–*18*).

The LHC is installed in a circular tunnel 27 km in circumference and 100 m underground, straddling the border between France and Switzerland, near Geneva (*19*). The LHC accelerates clockwise and counterclockwise beams of protons before colliding them head on. These collisions were at a total center-of-mass energy of 7 TeV in 2011 and 8 TeV in 2012, the highest energies reached to date in a particle accelerator. These high-energy collisions enable the production of new, and sometimes very heavy, particles by converting energy into mass in accordance with Einstein's well-known formula $E = mc^2$. The LHC can produce all known particles, including the top quark, which, with a mass of about 173 GeV, is the heaviest known elementary particle. It was predicted that the SM Higgs boson could also be produced at the LHC if it has a mass less than about 1 TeV.

The SM predicts the cross section for the production of Higgs bosons in proton-proton collisions as a function of its mass. The cross section increases with the center-of-mass energy of the collision and decreases with increasing Higgs mass. Despite the high collision energy, the predicted probability of Higgs boson production is extremely small, about 10^{-10} per collision. Thus, to detect a significant number of Higgs bosons a huge number of collisions must be analyzed, which requires very high luminosity. The maximum instantaneous luminosity achieved so far is 7.6×10^{33} cm^{-2} s^{-1}, close to the LHC peak design value that was not expected to be attained until 2015. This was achieved by having 1368 bunches of protons in each beam, spaced 50 ns apart (corresponding to a separation of about 16 m), with each bunch containing about 1.5×10^{11} protons squeezed to a transverse size of about 20 μm at the interaction point. Each bunch crossing yields more than 20 proton-proton collisions on average. The multiple collisions per bunch crossing, known as pileup, are initially registered as a single collision event by the detectors. Resolving the individual collisions within these events is an important challenge for the detectors at the LHC.

The Compact Muon Solenoid (CMS) detector surrounds one of the LHC's interaction points. Heavy particles, such as SM Higgs bosons, created in LHC collisions will typically be unstable and thus rapidly decay into lighter, more stable particles, such as electrons, muons, photons, and hadronic jets (clusters of hadrons travelling in a similar direction). These long-lived particles are what CMS detects and identifies, measuring their energies and momenta with high precision in order to infer the presence of the heavy particles produced in the collisions. Because the CMS detector is nearly hermetic, it also allows for the reconstruction of momentum imbalance in the plane transverse to the beams, which is an important signature for the presence of a neutrino (or a new, electrically neutral, weakly interacting particle) in the collision.

We report the observation of a new particle that has properties consistent with those of the SM Higgs boson. This paper provides an overview of the experiment and results that are described in greater detail in (*20*). The study examines five SM Higgs boson decay modes. Three modes result in pairs of bosons ($\gamma\gamma$, ZZ, or W^+W^-), and two modes yield pairs of fermions ($b\bar{b}$ or $\tau^+\tau^-$), where γ denotes a photon, Z and W denote the force carriers of the weak interaction, b denotes a bottom quark (and $\bar{b}$ its antiquark), and τ denotes a tau lepton. In the following, we omit the particle charges and use b to refer to both the quark and antiquark. The unstable W, Z, b, and τ particles decay to final states containing electrons, muons, neutrinos, and hadronic jets, all of which can be detected (directly or, in the case of neutrinos, indirectly) and measured with the CMS detector. An independent observation was made by the ATLAS collaboration (*21*, *22*), which further strengthens our interpretation.

Overview of the CMS detector. The CMS detector measures particles produced in high-energy proton-proton and heavy-ion collisions (*23*). The central feature of the detector is a superconducting solenoid 13 m long, with an internal diameter of 6 m. Within its volume it generates a uniform 3.8-T magnetic field along the axis of the LHC beams. Within the field volume are a silicon pixel and strip tracker, a lead tungstate ($PbWO_4$) scintillating crystal electromagnetic calorimeter, and a brass/scintillator hadron calorimeter (HCAL). Muons are identified and measured in gas-ionization detectors embedded in the outer steel magnetic-flux-return yoke. The detector is subdivided into a cylindrical barrel part and endcap disks on each side of the

*To whom correspondence should be addressed. E-mail: cms-spokesperson@cern.ch
†The complete list of authors and affiliations is available as supplementary material on *Science* Online.

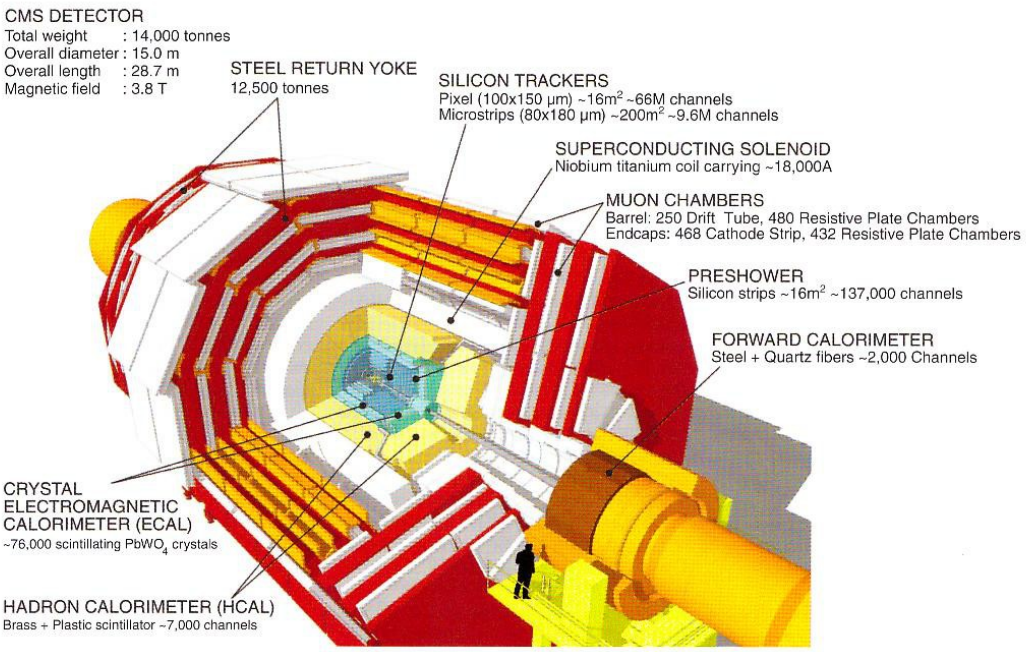

Fig. 1. Schematic view of the CMS detector showing its main components.

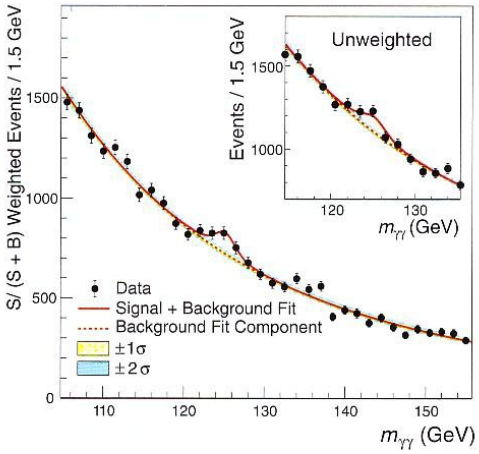

Fig. 2. Diphoton ($\gamma\gamma$) invariant mass distribution for the 7- and 8-TeV data collected by CMS in 2011 and 2012, respectively (black points with error bars). The data are weighted by the ratio of the signal to signal plus background for each event class. The solid red line shows the fit result for signal-plus-background; the dashed red line with color bands shows only the background with its uncertainties at 1σ (yellow) or 2σ (cyan). (**Inset**) The central part of the unweighted invariant mass distribution. Integrated luminosity was 5.1 fb^{-1} in 2011 and 5.3 fb^{-1} in 2012.

interaction point. Forward calorimeters complement the coverage provided by the barrel and endcap detectors. The CMS detector has a large angular acceptance, detecting particles over the full azimuthal range and with θ larger than 0.8°, where θ is the polar angle relative to the beam axis. Figure 1 shows the CMS detector and its main components.

The 66 million silicon pixels and 9.3 million silicon strips forming the tracker are used to determine the trajectories of charged particles. The multilayer silicon detectors provide accurate tracking of charged particles with excellent efficiency, which is especially important for the high-pileup conditions at the LHC. The magnetic field curves the trajectories of charged particles, allowing the measurement of their momenta. The track-finding efficiency is more than 99%, and the uncertainty in the measurement of transverse momentum, p_T (projection of the momentum vector onto the plane perpendicular to the beam axis), is between 1.5 and 3% for charged tracks of $p_T \sim 100$ GeV. By extrapolating tracks back toward their origins, the precise proton-proton interaction points, or collision vertices, can be determined. Decay vertices of long-lived particles containing heavy-quark flavors, such as B mesons, can similarly be identified and reconstructed. Such "b-tagging" is particularly useful in searches for previously unobserved particles, such as the Higgs boson.

The electromagnetic calorimeter (ECAL) absorbs photons and electrons. These produce showers of particles in the dense crystal material, which yield scintillation light detected by photodetectors glued to the rear faces of the 75,848 crystals. The amount of light detected is proportional to the energy of the incoming electron or photon, allowing their energies to be determined with a precision of about 1% in the region of interest for the analyses reported here. Because electrons are charged particles, they can be discriminated from photons by matching the ECAL signal with a track reconstructed in the tracker.

Hadrons can also initiate showers in the ECAL, but they generally penetrate further into

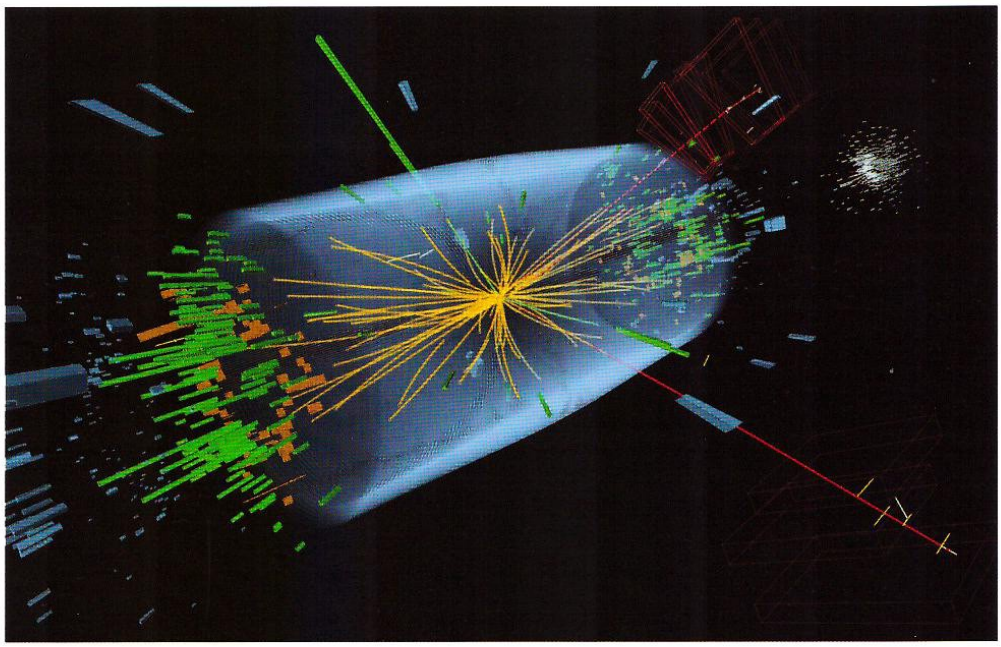

Fig. 3. Event recorded with the CMS detector in 2012 at a proton-proton center-of-mass energy of 8 TeV. The event shows characteristics expected from the decay of the SM Higgs boson to a pair of Z bosons, one of which subsequently decays to a pair of electrons (green lines in the tracker matched to green towers in the ECAL in the central region of the detector) and the other decays to a pair of muons (red lines). The event could also be due to known SM background processes.

the detector, reaching the HCAL surrounding the ECAL. The measurements of particle energies in the HCAL are not as precise as those of the ECAL but are well adapted to the needs of the CMS physics program.

The solenoid is surrounded by a large detector system that identifies and measures momenta of muons. It comprises three different types of gas-ionization detectors that enable muon momenta to be measured with a precision of less than 1% in the region of interest relevant for the search presented here.

The combination of information from all detectors is used to reconstruct the particle content in a collision event through an algorithm known as particle flow. The quarks and gluons, created in a hard collision of the constituents of the protons, combine and form jets of collimated hadrons in the detector. Once reconstructed from data, the jet energy is calibrated to provide an accurate measurement of the energy of the underlying quark or gluon. A vector sum of the momenta of all visible particles is computed, and the missing transverse momentum deduced from momentum conservation leads to the inference of the presence of undetected particles, such as neutrinos.

Although the LHC typically produces close to half a billion collisions in roughly 20 million bunch crossings per second, only a tiny fraction of these contain potentially interesting new phenomena, so it is neither necessary nor feasible to record all of the data from every single collision. CMS uses a two-level online trigger system to reduce the event rate from about 20 MHz to about 500 Hz, keeping only those events that are worthy of further investigation. The first level uses custom electronics close to the detector to analyze coarse information from the calorimeters and muon detectors to reduce the rate to 100 kHz or less. The second level uses a computing farm of 13,000 processor cores to analyze the full information from all subdetectors in order to make the final decision on whether to record an event. CMS has thus far selected several billion events, corresponding to more than 4 petabytes of stored event data. The recorded events are sent to computing centers at CERN and around the world to fully reconstruct the particles produced in each collision and allow subsequent analyses.

Searching for the SM Higgs boson. At the LHC, the SM Higgs boson should be produced most efficiently through gluon-gluon fusion: Gluons from each of the colliding protons fuse together to form a Higgs boson. Two additional important production processes are vector boson fusion (VBF), where quarks inside the protons emit W or Z bosons that fuse to form the Higgs boson, and associated production (VH), where a vector boson V (either a W or Z) is produced together with the Higgs boson. The interacting quarks in the VBF events also give rise to high-energy jets produced at small angles that can be detected and used to help identify this event type. Both VBF and VH events have better signal-to-background ratios relative to gluon fusion but occur far less frequently (*24–28*).

For every inverse femtobarn ($fb^{-1} = 10^{-39}$ cm^{-2}) of integrated luminosity at the LHC, about 20,000 SM Higgs bosons are expected to be produced if the Higgs mass is close to 125 GeV. The majority of these decay to final states that have large backgrounds, making identification difficult or impossible. Dedicated methods have been developed to exploit channels with lower decay fractions by selecting certain kinematical regions of the decay products where the signal-to-background ratio is sufficiently large to make the observation of SM Higgs bosons possible. Extensive use is made of particle-isolation criteria to reject the high-rate jet background, because, in general, the particles from Higgs decays appear relatively isolated from each other and other particles in the detector.

Billions of detailed simulated events have been generated to develop and refine the analysis

techniques needed to estimate the SM Higgs boson signals and backgrounds (*29*–*32*). Samples of simulated events reconstructed with the same software as used for the LHC data allow, for example, the estimation of background yields or the prediction of the expected significance for the observation of new particles. However, in the presented analyses the background estimations are derived mostly from the control samples in data.

We studied five SM Higgs decay modes: $H\rightarrow\gamma\gamma$, $H\rightarrow ZZ$, $H\rightarrow WW$, $H\rightarrow\tau\tau$, and $H\rightarrow bb$. The $\gamma\gamma$, ZZ, and WW channels are of comparable sensitivity in the search for a Higgs boson with a mass around 125 GeV and are more sensitive than the bb and $\tau\tau$ channels. Both the $\gamma\gamma$ and ZZ channels provide precise mass measurements of the parent particle. The presence of an SM Higgs boson decaying to these final states would appear as relatively narrow peaks in the invariant mass spectra of $\gamma\gamma$ and ZZ.

An integrated luminosity of 5.1 fb^{-1} was collected by CMS in 2011 at 7 TeV, allowing a first thorough investigation into the existence, or nonexistence, of the SM Higgs boson over a wide mass range. This led to CMS's first significant exclusion of the SM Higgs boson in the medium- and high-mass region between 127 and 600 GeV (*33*–*38*). Data from the ATLAS experiment excluded a similar region (*39*). This left a small window where a low-mass SM Higgs boson could still exist.

In the low-mass region below 127 GeV, the 2011 data analyses also showed an excess over the background-only expectation in the vicinity of 124 GeV. ATLAS observed a similar excess at around the same mass value (*39*). The observed excess in CMS was inconclusive, being around three standard deviations (3σ) above the background-only expectation. After taking into account the possibility that a signal-like excess could appear randomly in the data between 110 and 145 GeV (the look-elsewhere effect), this significance was reduced to about 2σ. Therefore, there was still a nonnegligible chance that this excess could be due to a random upward fluctuation in the background, making it look like a signal. More data were needed to establish whether this excess was genuine or not. It was predicted that, in the case of a Higgs boson signal, around 10 fb^{-1} more data would be required to reach a statistical significance of around 5σ. However, the LHC operation at 8 TeV in 2012 (giving a 20% increase in Higgs boson production cross section compared to 7 TeV), coupled with improved analyses with 20 to 30% higher sensitivity, reduced this additional required luminosity to around 5 fb^{-1}. By the summer of 2012, CMS had collected an additional 5.3 fb^{-1} of collision data at this new energy.

Because the 2011 analysis (*33*–*38*) showed an excess of events at about 125 GeV and to avoid a potential bias in the choice of selection criteria for the 2012 data that might artificially enhance this excess, we performed the analysis of the 2012 data "blind": The region where the signal may be present was not examined until after all the analysis criteria had been fully scrutinized and agreed upon within the collaboration.

Search for the SM Higgs boson decay into two photons. The predicted probability for a 125-GeV SM Higgs boson to decay into two photons is about 0.3%. Yet this decay mode is one of the most important, because both photons can be measured very accurately in the CMS ECAL and the backgrounds can be precisely estimated. The presence of a signal would manifest itself as a narrow peak above a smoothly falling background in the invariant mass distribution of the two photons.

The energy resolution and precise knowledge of the absolute energy scale of the ECAL are key elements of this analysis. These were achieved by calibrating each channel of the ECAL in situ, using diphoton decays of π^0 and η^0, for example. The stability of the ECAL response was ensured by the use of a sophisticated real-time monitoring procedure that corrects any deviations with a precision of a few per mill. Decays of Z bosons into electron pairs were then used to determine the energy resolution and energy scale, taking advantage of the precise knowledge of the Z mass and width.

An additional challenge is to determine from which of the many collision vertices in the event the two photons originate, which affects the precision of the mass measurement of the parent particle. The collisions occurring in a single LHC bunch crossing, as many as 40 in 2012, are spread over a distance of about 10 cm along the beam axis at the center of CMS. Because photons do not leave tracks in the detector, there can be ambiguity as to which collision vertex they belong to. A variety of techniques were used to determine the diphoton vertex, including use of event kinematics and an understanding of photon conversions into electron pairs.

Multivariate analyses (*40*, *41*) based on boosted decision trees were used to identify the photons and to extract their energies and uncertainties on a photon-by-photon basis. To optimize sensitivity, we categorized diphoton events into four classes with decreasing restrictions on the quality according to many variables, including the uncertainty on the diphoton mass measurement, the kinematics of the photons, and whether the photons convert into electron pairs in the material before reaching the ECAL. For example, events where both photons are in the central region of CMS and do not convert into electron pairs in the tracker were given the highest classification because they are the most precisely measured. We also included additional classes for diphoton events that have two additional jets with properties consistent with those expected for the VBF production process.

Photons of high quality (determined from the spatial distribution of electromagnetic showers and isolation criteria) were selected with energies above 30 to 40 GeV, depending on the event class. Figure 2 shows the diphoton invariant mass spectrum from all the data collected by CMS from 2011 to mid-2012, after selections as defined in (*20*). The spectrum was built up from the event classes, with each class weighted by the ratio of the signal to signal-plus-background estimated from simulation. An excess was observed at 125 GeV on an otherwise smoothly falling background spectrum. The background consists mostly of collisions where two photons are produced in SM processes and a smaller fraction from events where at least one of the photon signals is not genuine but originates from the debris of jets.

The observed excess is consistent in shape and size with that expected for diphoton decays

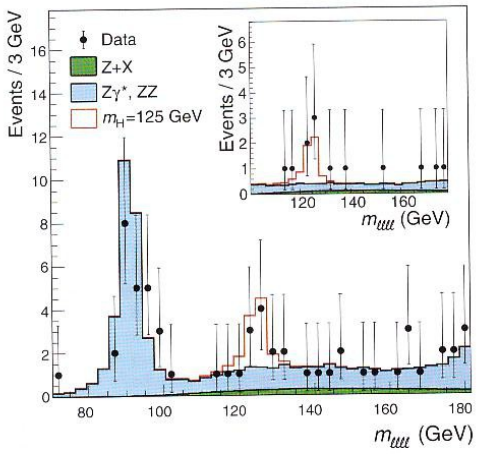

Fig. 4. Distribution of the four-lepton reconstructed invariant mass for the sum of the 4e, 4μ, and 2e2μ channels. Points represent the data, shaded histograms represent the background, and the empty histogram the signal expectations. The distributions are presented as stacked histograms. The measurements are presented for the sum of the data collected at center-of-mass energies of 7 and 8 TeV during 2011 and 2012, respectively. Error bars represent standard deviations. **(Inset)** The four-lepton invariant mass distribution after selection of events with signal-like kinematics, as described in the text.

of SM Higgs bosons. To evaluate the significance of the signal, we fitted the background spectrum over the whole mass range with a fifth-order polynomial function (or a third-order polynomial for the VBF categories) and measured the magnitude of the excess above the background. The diphoton decay mode has a signal significance of 4.1σ relative to the background-only hypothesis. This excess is present in both 2011 and 2012 data and is consistent between the two data sets.

The observation of the diphoton final state also implies that the new particle is a boson and has an integer spin different from unity (*42*, *43*).

Search for the SM Higgs boson decay into two Z bosons. If the SM Higgs boson has a mass of 125 GeV, about 2.6% of them are predicted to decay into two Z bosons. At least one of the Z bosons is necessarily virtual, that is, it has a different mass than the 91 GeV Z mass. The Z bosons each decay into pairs of leptons or quarks. We concentrate on the Z decays into leptons, particularly electrons (e) and/or muons (μ), because these have the smallest SM backgrounds. In CMS, we analyzed separately the three different final states in this channel, namely 2e2μ, 4e, and 4μ, and then combined the results.

The invariant mass of the ZZ system can be reconstructed and measured with good accuracy in CMS from the four-lepton momenta. Hence, the presence of a Higgs boson in the data should manifest itself as a peak in the ZZ invariant mass spectrum in the presence of a small continuum background.

There are numerous SM processes (not including Higgs boson decays) that can lead to the same final states. They include direct ZZ production from quark-antiquark annihilation and gluon-gluon fusion, as well as processes involving a single Z boson produced with associated heavy-quark jets and top-antitop pair-production. Apart from the rate of direct ZZ production, which we can determine accurately from simulation, the rates of other backgrounds were extracted from data.

The leptons from Z decays are, in general, well isolated in the detector; that is, their trajectories are far from the debris of jets or other particles produced in the collision. Despite the large particle multiplicity per event from pileup interactions, the overall efficiency for selecting isolated leptons remains very high.

We selected collisions with four isolated leptons originating from the same vertex, for which the transverse momentum of each muon is at least 5 GeV and of each electron is at least 7 GeV. (These criteria were determined by using a large sample of single-Z events collected in the past 2 years.) Both Z boson candidates are required to decay to two same-flavor leptons of opposite charge, and the invariant mass of the dileptons produced in the Z boson decays must be in the range from 40 to 120 GeV for the heavier of the two and 12 to 120 GeV for the lighter one.

Figure 3 shows a typical event containing two reconstructed Z bosons, with a ZZ invariant mass around 125 GeV. The ZZ invariant mass spectrum for selected events is shown in Fig. 4. Because leptons (especially electrons) can often radiate an energetic photon at an early stage of their trajectory through the detector, the energy or momentum of such leptons can be considerably underestimated. We therefore searched for energetic photons close to these leptons and added their energies when appropriate.

The invariant mass spectrum in Fig. 4 shows a Z peak at 91 GeV resulting from decays of Z bosons into two leptons and an energetic virtual photon that materializes through a second dilepton pair. There is also a statistically significant peak near 125 GeV. This completely independent analysis indicates the presence of a signal in the same region as that found in the diphoton decay mode. This is to be expected if indeed the signals correspond to the same parent particle.

The signal-to-background separation improves further by exploiting the decay kinematics expected for signal events, especially the decay angles and invariant masses of the two pairs of leptons (*44*). Analyzing events in the peak at 125 GeV confirmed that many of these events have the requisite characteristics; this reinforced our interpretation that the signal is genuine. The statistical significance of the excess observed by combining data from 2011 and 2012, accounting also for the decay-angle characteristics, is 3.2σ relative to the background-only hypothesis. The maximum significance occurs at a mass of 125.6 GeV.

Search for Higgs boson decays in other channels. Apart from the γγ and ZZ channels discussed above, CMS also searched for decays of SM Higgs bosons to two W bosons, two τ leptons, or two b quarks.

For the WW decay mode, the final states must contain two opposite-sign leptons (either electrons or muons) and significant missing transverse momentum, resulting from the undetected neutrinos from W decays. In contrast to the γγ and ZZ modes, the invariant mass of the two W bosons cannot be precisely reconstructed. The potential excess in the data over the background expectation provides only a continuum instead of a sharp resonance peak. We used multivariate analysis techniques to optimize the sensitivity to a possible signal present in data. We classified the events into a number of exclusive categories, for example, according to lepton flavor content and whether there are jets present (to enhance VBF production relative to gluon fusion).

These different event classes were subject to different backgrounds and have different sensitivities. The challenge for this analysis was to estimate the backgrounds from the SM, which was generally achieved through techniques based on control regions in the data and complemented through simulation. Special attention was paid to determining the missing transverse momentum, particularly in the presence of large pileup (as in the 2012 data sample).

We selected events in which the p_T of the most energetic lepton is greater than 20 GeV and that of the second-most-energetic lepton is above 10 GeV and that have missing transverse momentum typically above 20 GeV. The results of this analysis, combining all the classes across the 2011 and 2012 data, show (Fig. 5) a broad excess of events over the expected background, consistent with the presence of a new particle at a mass near 125 GeV. The statistical significance is about 1.5 to 2.0σ relative to the background-only hypothesis.

We also explored whether this new particle decays into fermion pairs, as it would be expected to if the associated field gives mass to the fermions in addition to the W and Z bosons, by

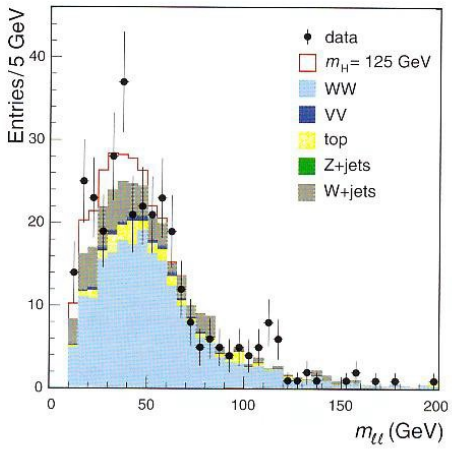

Fig. 5. Distribution of the invariant mass of lepton pairs for the zero-jet eμ category in the search at 8 TeV for the SM Higgs boson decay to a pair of W bosons. The signal expected from the SM Higgs boson with a mass m_H = 125 GeV is shown added to the background. Error bars indicate standard deviations.

looking for instances where the particle decays into heavy fermions. The heaviest fermions into which a 125-GeV SM Higgs boson can decay are the τ leptons and b quarks.

The detection of τ leptons is challenging because they are unstable and decay less than 10^{-12} s after production, either into a lighter charged lepton (electron or muon) and neutrinos or into a neutrino and either one or three charged pions possibly accompanied by neutral pions. CMS has tools to detect and reconstruct such decays and separate these from backgrounds. Several decay channels were explored, including the combination of one τ lepton decaying exclusively into leptons and the other into hadrons. A natural process to calibrate the analysis is through Z boson production, where 3.4% of the Z decays are into $\tau^+\tau^-$ pairs, and CMS has successfully used this decay channel (*45*).

The main challenge for this search is to assess the backgrounds, most of which are extracted using control samples in data. Different τ decay channels are analyzed separately and classified accordingly, including classes with accompanying jets. The results of these individual analyses were then combined for a final result.

As in the case of the WW decay mode, the presence of neutrinos in the decay products of the τ leptons prevents a full event reconstruction, and, instead of a resonance peak, a broad enhancement over background is expected. We have not yet found such an enhancement, but the current sensitivity to this channel does not exclude the presence of the SM Higgs boson. With the LHC on course to triple the integrated luminosity by the end of 2012, studies of the ττ channel will become more sensitive.

Lastly, CMS conducted a search for SM Higgs bosons decaying into two b quarks. Each quark gives rise to a jet that is recognized in the analysis ("tagged") as originating from b quarks. For the tagging of b quarks, we searched for secondary vertices in the jets, caused by decays of B hadrons that travel a few millimeters before decaying. The energy of the original b quark is estimated from the energies of all the particles in its jet and has a large uncertainty. The reconstructed masses of objects obtained from these jets are therefore expected to be distributed over a region of about 20 GeV in the mass range of interest.

At low mass (below about 135 GeV), the SM Higgs boson decay into b quarks has the largest rate of the five search modes we report in this paper, and we therefore expect a large number of such decays in the data. This signal is, however, overwhelmed by a large background from SM b quark production, making the search less sensitive. To have a more favorable signal-to-background ratio, we searched for this signal in the (rarer) associated production process involving a W or Z boson, which can be detected from their leptonic decays. We required these bosons to have transverse momenta above 50 GeV.

To minimize the background in the bb channel, we again used several mutually exclusive classes of events, which were analyzed separately. These classes are based on the transverse momentum of the jet pair and the nature and decay of the associated boson. For the final result, we combined all these channels and used all of the available data from 2011 and 2012. The result shows a small excess above the background-only expectation over a large mass range, including the region near 125 GeV. The sensitivity of this analysis is about 1.5 times lower than required for concluding whether a signal is present (as expected from SM prediction) or if the coupling to b quarks is different from what we would expect. Again, tripling the amount of collision data should be decisive.

In conclusion, neither fermion decay mode shows, at present, a statistically significant enhancement over the background-only expectation. Nevertheless, at the present level of sensitivity the results in these channels are consistent with the production of the SM Higgs boson, in agreement with observations in the other three (diboson) decay modes.

Observation of a new particle. The final result combines all the information collected through a global fit (*46*) to the five different search channels. The result reflects the probability for the background to deviate from the expectation by at least the observed amount, assuming the absence of the SM Higgs boson in this mass range. This probability, known as the local *P* value, is evaluated by using sets of simulated data that incorporate all experimental uncertainties and correlations among analyses. The result is shown (Fig. 6) for each of the five search channels individually, as well as for the combination of all five channels. For the combination the minimum *P* value at 125 GeV is of the order of one in three million.

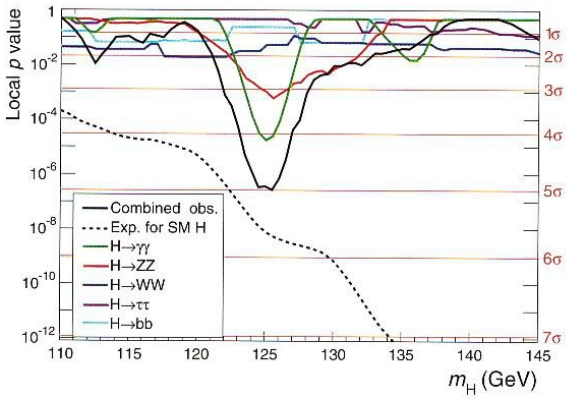

Fig. 6. The observed probability (local *P* value) that the background-only hypothesis would yield as many (or more) events as seen in the CMS data, as a function of the mass of the SM Higgs boson for each of the five search channels individually and the combination of all five channels. The dashed line shows the median expected local *P* values for the SM Higgs boson with a mass m_H.

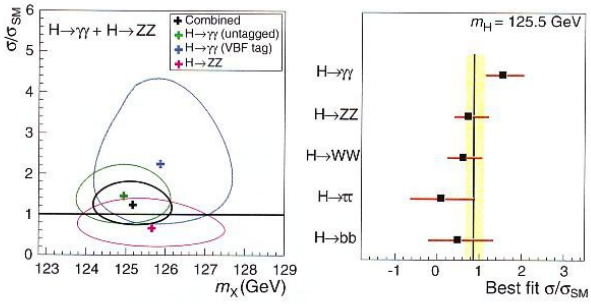

Fig. 7. (Left) 68% CL contours for the relative signal strength σ/σ_{SMH} versus the Higgs boson mass for the high-precision decay modes (γγ and ZZ). **(Right)** The relative signal strength σ/σ_{SMH} for the five Higgs boson decay modes examined by CMS. The symbol σ/σ_{SM} denotes the production cross section multiplied by the relevant branching fraction, relative to the SM expectation.

This probability corresponds to a local significance of 5σ. The probability of observing this large a fluctuation anywhere in the mass range of 114 to 130 GeV, where the Higgs boson had not been excluded by previous data, is small and results in a global significance of 4.6σ. The global significance is smaller than the local value because of the look-elsewhere effect. Both measures convincingly show that this is not a background fluctuation, but rather the observation of a new particle. The expected sensitivity with the present data for a 125 GeV SM Higgs boson amounts to a local significance of 5.8 ± 1.0σ, consistent with the signal observed at 5σ.

In addition to being able to say with high confidence that a new particle has been observed, and that it is a boson with spin not equal to one, we were also able to derive some of its properties, such as its mass. And, as mentioned above, once the mass is known the SM allows us to calculate many other properties, such as the fractions of Higgs bosons decaying in different ways, and compare these expectations with our measurements. This is expressed as the signal strength, that is, the measured production rate of the signal, which can be determined for each decay mode individually and for the overall combination of all channels, normalized to the predicted Higgs boson production rate. The signal strength was defined to be equal to one for the SM Higgs boson. The measured signal strength was highest in the diphoton channel, namely 1.6 ± 0.4, whereas that in the ZZ channel was $0.7^{+0.4}_{-0.3}$. By using the high-resolution diphoton and ZZ channels discussed above, which show a resonance peak, we obtained the 68% confidence level (CL) contours for the signal strength versus the boson mass (Fig. 7 left). We also show the combination of the diphoton and ZZ decay modes, where the relative signal strengths of these two modes are constrained by the expectations for the SM Higgs boson. To extract the value of the mass in a model-independent way, we allowed the signal yields of the combined channels to vary independently. The combined best-fit mass is 125.3 ± 0.4 (statistical) ± 0.5 (systematic) GeV.

The signal strengths for all five channels are depicted in Fig. 7 (right). The overall combined signal strength, including all channels, is 0.87 ± 0.23. Hence, these results are consistent, within relatively large statistical and systematic uncertainties, with the expectations for the SM Higgs boson.

The CMS data also rule out the existence of the SM Higgs boson in the ranges of 114.4 to 121.5 GeV and 128 to 600 GeV at 95% CL (*20*). Lower masses were already excluded by CERN's Large Electron Positron collider at the same CL (*14*).

More data are needed to establish whether this new particle has all the properties of the SM Higgs boson or whether some do not match. The latter may imply new physics beyond the SM. This particle has the potential to be a portal to a new landscape of physical phenomena that is still hidden from us. The CMS experiment is in an excellent position to undertake this research in the years to come.

References and Notes

1. S. L. Glashow, *Nucl. Phys.* **22**, 579 (1961).
2. S. Weinberg, *Phys. Rev. Lett.* **19**, 1264 (1967).
3. A. Salam, in *Elementary Particle Physics: Relativistic Groups and Analyticity*, N. Svartholm, Ed. (Nobel Symposium 8, Almqvist and Wiskell, Stockholm, 1968), pp. 367–377.
4. F. Englert, R. Brout, *Phys. Rev. Lett.* **13**, 321 (1964).
5. P. W. Higgs, *Phys. Lett.* **12**, 132 (1964).
6. P. W. Higgs, *Phys. Rev. Lett.* **13**, 508 (1964).
7. G. S. Guralnik, C. R. Hagen, T. W. B. Kibble, *Phys. Rev. Lett.* **13**, 585 (1964).
8. P. W. Higgs, *Phys. Rev.* **145**, 1156 (1966).
9. T. W. B. Kibble, *Phys. Rev.* **155**, 1554 (1967).
10. J. M. Cornwall, D. N. Levin, G. Tiktopoulos, *Phys. Rev. Lett.* **30**, 1268 (1973).
11. J. M. Cornwall, D. N. Levin, G. Tiktopoulos, *Phys. Rev. D* **10**, 1145 (1974).
12. C. H. Llewellyn Smith, *Phys. Lett. B* **46**, 233 (1973).
13. B. W. Lee, C. Quigg, H. B. Thacker, *Phys. Rev. D Part. Fields* **16**, 1519 (1977).
14. ALEPH, DELPHI, L3, OPAL Collaborations, and LEP Working Group for Higgs Boson Searches, *Phys. Lett. B* **565**, 61 (2003).
15. T. Aaltonen *et al.*; CDF Collaboration; D0 Collaboration, *Phys. Rev. Lett.* **104**, 061802 (2010).
16. CDF Collaboration, "Combined search for the standard model Higgs boson decaying to a bb pair using the full CDF data set" (2012), http://arxiv.org/abs/1207.1707.
17. T. Aaltonen *et al.*; CDF Collaboration; D0 Collaboration, *Phys. Rev. Lett.* **109**, 071804 (2012).
18. D0 Collaboration, "Combined search for the standard model Higgs boson decaying to *bb* using the D0 Run II data set" (2012), http://arxiv.org/abs/1207.6631.
19. L. Evans, P. Bryant, *J. Instrum.* **3**, S08001 (2008).
20. CMS Collaboration, *Phys. Lett. B* **716**, 30 (2012).
21. ATLAS Collaboration, *Phys. Lett. B* **716**, 1 (2012).
22. ATLAS Collaboration, *Science* **338**, 1576 (2012).
23. CMS Collaboration *et al.*, *J. Instrum.* **3**, S08004 (2008).
24. J. R. Ellis, M. K. Gaillard, D. V. Nanopoulos, *Nucl. Phys. B* **106**, 292 (1976).
25. H. M. Georgi, S. L. Glashow, M. E. Machacek, D. V. Nanopoulos, *Phys. Rev. Lett.* **40**, 692 (1978).
26. S. L. Glashow, D. V. Nanopoulos, A. Yildiz, *Phys. Rev. D* **18**, 1724 (1978).
27. S. Alioli, P. Nason, C. Oleari, E. Re, *J. High Energy Phys.* **0904**, 002 (2009).
28. P. Nason, C. Oleari, *J. High Energy Phys.* **1002**, 37 (2010).
29. T. Sjöstrand, S. Mrenna, P. Z. Skands, *J. High Energy Phys.* **0605**, 026 (2006).
30. S. Gieseke *et al.*, "Herwig++ 2.0 Release Note" (2006), http://arxiv.org/abs/hep-ph/0609306.
31. J. Alwall *et al.*, *J. High Energy Phys.* **0709**, 028 (2007).
32. S. Agostinelli *et al.*, *Nucl. Instrum. Meth. A* **506**, 250 (2003).
33. CMS Collaboration, *Phys. Lett. B* **710**, 26 (2012).
34. CMS Collaboration, *Phys. Lett. B* **710**, 403 (2012).
35. CMS Collaboration, *Phys. Rev. Lett.* **108**, 111804 (2012).
36. CMS Collaboration, *Phys. Lett. B* **710**, 91 (2012).
37. CMS Collaboration, *Phys. Lett. B* **713**, 68 (2012).
38. CMS Collaboration, *Phys. Lett. B* **710**, 284 (2012).
39. ATLAS Collaboration, *Phys. Rev. D* **86**, 032003 (2012).
40. H. B. Prosper, paper presented at XII International Workshop on Advanced Computing and Analysis Techniques in Physics Research (ACAT08), 3 to 7 November 2008, Erice, Italy, no. PoS(ACAT08)010.
41. P. C. Bhat, *Annu. Rev. Nucl. Part. Sci.* **61**, 281 (2011).
42. L. D. Landau, *Dokl. Akad. Nauk* **60**, 207 (1948).
43. C. N. Yang, *Phys. Rev.* **77**, 242 (1950).
44. CMS Collaboration, *J. High Energy Phys.* **4**, 36 (2012).
45. CMS Collaboration, *J. High Energy Phys.* **08**, 117 (2011).
46. ATLAS and CMS Collaborations, technical report ATL-PHYS-PUB 2011-11, CMS NOTE 2011/005 (2011), http://cdsweb.cern.ch/record/1379837.

Acknowledgments: We congratulate our colleagues in the CERN accelerator departments for the excellent performance of the LHC machine. We thank the computing centers in the Worldwide LHC Computing Grid for the provisioning and excellent performance of computing infrastructure essential to our analyses and the administrative staff at CERN and the other CMS institutes. We gratefully acknowledge the contributions of the technical staff at CERN and other CMS institutes and the support from all the funding agencies that contributed to the construction and the operation of the CMS detector: the Austrian Federal Ministry of Science and Research; the Belgian Fonds de la Recherche Scientifique, and Fonds voor Wetenschappelijk Onderzoek; the Brazilian funding agencies [Conselho Nacional de Desenvolvimento Cientifico e Technologico(CNPq), Coordenação de Aperfeiçoamento de Pessoal de Nível Superior (CAPES), Fundação de Amparo à Pesquisa do Estado do Rio de Janeiro (FAPERJ), and Fundação de Amparo à Pesquisa do Estado do Sao Paulo (FAPESP)]; the Bulgarian Ministry of Education, Youth, and Science; CERN; the Chinese Academy of Sciences, Ministry of Science and Technology, and National Natural Science Foundation of China; the Colombian funding agency (COLCIENCIAS, Departamento Administrativo de Ciencia, Tecnología, e Innovación); the Croatian Ministry of Science, Education, and Sport; the Research Promotion Foundation, Cyprus; the Ministry of Education and Research, Recurrent financing contract SF0690030s09 and European Regional Development Fund, Estonia; the Academy of Finland, Finnish Ministry of Education and Culture, and Helsinki Institute of Physics; the Institut National de Physique Nucléaire et de Physique des Particules–CNRS, and Commissariat à l'Énergie Atomique et aux Énergies Alternatives–CEA, France; the Bundesministerium für Bildung und Forschung, Deutsche Forschungsgemeinschaft, and Helmholtz-Gemeinschaft Deutscher Forschungszentren, Germany; the General Secretariat for Research and Technology, Greece; the National Scientific Research Foundation, and National Office for Research and Technology, Hungary; the Department of Atomic Energy and the Department of Science and Technology, India; the Institute for Studies in Theoretical Physics and Mathematics, Iran; the Science Foundation, Ireland; the Istituto Nazionale di Fisica Nucleare, Italy; the Korean Ministry of Education, Science and Technology and the World Class University program of NRF, Republic of Korea; the Lithuanian Academy of Sciences; the Mexican funding agencies [Centro de Investigación y Estudios Avanzados, (CINVESTAV), Consejo Nacional de Ciencia y Technología (CONACYT), Secretaría de Educación Pública (SEP), and Universidad Autónoma de San Luis Potosí Fondo de Apoyo a la Investigación (UASLP-FAI)]; the Ministry of Science and Innovation, New Zealand; the Pakistan Atomic Energy Commission; the Ministry of Science and Higher Education and the National Science Centre, Poland; the Fundação para a Ciência e a Tecnologia, Portugal; JINR (Joint Institute for Nuclear Research) (Armenia, Belarus, Georgia, Ukraine, Uzbekistan); the Ministry of Education and Science of the Russian Federation, the Federal Agency of Atomic Energy of the Russian Federation, Russian Academy of Sciences, and the Russian Foundation for Basic Research; the Ministry of Science and Technological Development of Serbia; the Secretaría de Estado de Investigación, Desarrollo, e Innovación and Programa Consolider-Ingenio 2010, Spain; the Swiss funding agencies [Eidgenössische Technische Hochschule (ETH) Board, ETH Zürich, Paul Scherrer Institut (PSI), Swiss National Science Foundation, Universität Zürich, Canton Zürich, and State Secretariat for Education and Research (SER)]; the National Science Council, Taipei; the Thailand Center of Excellence in Physics, the Institute for the Promotion of Teaching Science and Technology of Thailand and the National Science and Technology Development Agency of Thailand; the Scientific and Technical Research Council of Turkey, and Turkish Atomic Energy Authority; the Science and Technology Facilities Council, UK; U.S. Department of Energy, and NSF.

Supplementary Materials

www.sciencemag.org/cgi/content/full/338/6114/1569/DC1
Complete Author List

10.1126/science.1230816

CMS collaboration

ARMENIA
Yerevan: Yerevan Physics Inst.

AUSTRIA
Wien: HEPHY

BELARUS
Minsk: Byelorussian State Univ.; National Centre for Part. and HEP; Research Inst. for Nuclear Problems; Research Inst. of Applied Physical Problems

BELGIUM
Antwerpen: Univ. Antwerpen;
Brussel: Vrije Univ. Brussel;
Bruxelles: Univ. Libre de Bruxelles;
Ghent: Ghent Univ.;
Louvain-la-Neuve: Univ. Catholique de Louvain;
Mons: Univ. de Mons-Hainaut

BRAZIL
Rio de Janeiro: Centro Brasileiro de Pesquisas Fisicas; Univ. do Estado do Rio de Janeiro;
Sao Paulo: Inst. de Fis. Teorica, Univ. Estadual Paulista (UNESP)

BULGARIA
Sofia: Inst. of System Engineering and Robotics; Univ. of Sofia; Inst. for Nucl. Research and Nucl. Energy;

CHINA
Beijing: Inst. of High Energy Phys.; SKLNPT, Peking Univ.;
Hefei: Univ. for Science & Tech. of China;
Shanghai: Shanghai Inst. of Ceramics

COLOMBIA
Bogota: Univ. de Los Andes (UNIANDES)

CROATIA
Split: Tech. Univ. of Split; Univ. of Split;
Zagreb: Inst. Rudjer Boskovic

CYPRUS
Nicosia: Univ. of Cyprus

CZECH Republic
Prague: Charles University

EGYPT
Cairo: Academy of Scientific Research and Technology of the Arab Republic of Egypt, Egyptian Network of High Energy Physics

ESTONIA
Tallinn: Nat. Inst. of Chemical Phys. and Biophys.

FINLAND
Helsinki: Dept of Physics, Univ. of Helsinki; Helsinki Inst. of Physics;
Lappeenranta: Lappeenranta Univ. of Technology

FRANCE
Villeurbanne: Univ. de Lyon, Univ. Claude Bernard Lyon 1, CNRS-IN2P3, Inst. de Physique Nucléaire; Centre de Calcul de l'Inst. Nat. de Phys. Nucl. et de Phys. des Part. (IN2P3)
Annecy-le-Vieux: LAPP, IN2P3-CNRS;
Gif-sur-Yvette: DSM/IRFU, CEA/Saclay;
Palaiseau: LLR, Ecole Polytechnique, IN2P3-CNRS;
Strasbourg: IPHC, Uni. Strasbourg, UHA Mulhouse - CNRS/IN2P3;

GEORGIA
Tbilisi: Inst. of High Energy Phys. and Informatization; Inst. of Physics, Academy of Science

GERMANY
Aachen: RWTH Aachen Univ., I. Physik. Inst.; RWTH Aachen Univ.,III. Physik. Inst. A; RWTH Aachen Univ.,
Hamburg: DESY; Univ. of Hamburg;
Karlsruhe: Inst. für Exp. Kernphysik

GREECE
Aghia Paraskevi: Inst. of Nucl. Phys. "Demokritos";
Athens: Univ. of Athens;
Ioánnina: Univ. of Ioánnina

HUNGARY
Budapest: KFKI Research Inst. for Part. & Nucl. Phys.;
Debrecen: Inst. of Nuclear Research ATOMKI; Univ. of Debrecen

INDIA
Chandigarh: Panjab Univ.;
Delhi: Univ. of Delhi;
Mumbai: Bhabha Atomic Research Centre; TIFR - EHEP; TIFR - HECR
Kolkata: Saha Inst. of Nucl. Ph.;

IRAN
Tehran: Inst. for Studies in Theoretical Physics & Math. (IPM)

IRELAND
Dublin: Univ. College Dublin

ITALY
Bari: INFN, Univ., Polit. di Bari;
Bologna: INFN, Univ. di Bologna;
Catania: INFN, Univ. di Catania;
Firenze: INFN, Univ. di Firenze;
Frascati: INFN Lab. Naz. di Frascati;
Genova: INFN Univ. di Genova;
Milano: INFN, Univ. di Milano-Biccoca;
Napoli: INFN, Univ. di Napoli "Federico II";
Padova: INFN, Univ. di Padova, Uni. Trento;
Pavia: INFN, Univ. di Pavia;
Perugia: INFN, Univ. di Perugia;
Pisa: INFN, Univ., Scuola Norm. Sup. di Pisa;
Roma: INFN, Univ. di Roma;
Torino: INFN, Univ. di Torino, Univ. del Piemonte Orientale;
Trieste: INFN, Univ. di Trieste

KOREA
Chonju: Chunbuk National Univ.;
Chunchon: Kangwon National Univ.;
Daegu: Kyungpook Univ.;
Iksan: Wonkwang Univ.;
Jeju: Cheju National Univ.;
Kwangju: Chonnam National Univ.;
Naju: Dongshin Univ.;
Namwon: Seonam Univ.;
Seoul: Uni. of Seoul, Konkuk Univ.; Korea Univ.;
Seoul National Univ.; Seoul National Univ. of Education;
Suwon: Sungkyunkwan Univ.

LITHUANIA
Vilnius: Lithuanian Acad. of Sciences; Vilnius Univ.

MEXICO
Mexico City: Centro de Investigacion IPN; Univ. Iberoamericana;
Puebla: Benemerita Univ. Autonoma de Puebla;
San Luis Potosi: Univ. Autonoma de San Luis Potosi (UASLP)

NEW ZEALAND
Auckland: Univ. of Auckland;
Christchurch: Univ. of Canterbury

PAKISTAN
Islamabad: National Centre for Physics, Quaid-I-Azam Univ.;
Rawalpindi Cantt: National Univ. of Sciences and Tech.

POLAND
Warsaw: Inst. of Exp. Phys.; Soltan Inst. for Nucl. Studies; Warsaw Univ. of Technology, ISE

PORTUGAL
Lisboa: Lab. of Instrum. and Exp. Part. Phys. (LIP)

RUSSIA
Moscow: Inst. for Nucl. Research; Inst. for Theoretical and Exp. Phys.; Moscow State Univ.;
Research & Development Inst. of Power Engineering;
Gatchina (*St. Petersburg*): Petersburg Nucl. Phys. Inst.;
Dubna: JINR;
Protvino: State Res. Center of Russian Fed., Inst. for High Energy Phys.;
St Petersburg: Electron Nat. Research Inst.;
Zhukovsky: Myasishchev Design Bureau

SERBIA
Belgrade: Vinca Inst. of Nucl. Sciences

SPAIN
Madrid: CIEMAT; Univ. Autónoma de Madrid;
Oviedo: Univ. de Oviedo;
Santander: IFCA, CSIC-Univ. de Cantabria

SWITZERLAND
Geneva: CERN;
Villigen: Paul Scherrer Inst.;
Zurich: ETH Zurich; Univ. Zu rich

TAIWAN
Chung-Li: National Central Univ.;
Taipei: National Taiwan Univ.

THAILAND
Bangkok: Chulalongkorn University

TURKEY
Adana: Cukurova Univ.;
Ankara: Middle East Technicak Univ.;
Istanbul: Bogaziçi Univ., Istanbul Tech. Univ

UKRAINE
Kharkov: Inst. of Single Crystals;
Kharkov Inst. of Phys. and Tech.; Kharkov State Univ.

UNITED KINGDOM
Bristol: Univ. of the West of England; Univ. of Bristol;
Didcot: RAL;
London: Imperial College;
Uxbridge: Brunel Univ.

USA
Davis: UC Davis;
La Jolla: UC San Diego;
Lubbock: Texas Tech Univ.;
Tallahassee: Florida State Univ.;
Santa Barbara: UC Santa Barbara;
Pasadena: California Inst. of Tech.;
Miami: Florida International Univ.;
Batavia: Fermi National Accelerator Lab.;
Los Angeles: UCLA;
Riverside: UC Riverside;
Fairfield: Fairfield Univ.;
Boston: Boston Univ.; Northeastern Univ.;
Providence: Brown Univ.;
Madison: Univ. of Wisconsin
Detroit: Wayne State Univ.;
Nashville: Vanderbilt Univ.;
Pittsburgh: Carnegie Mellon Univ.;
Chicago: Univ. of Illinois at Chicago;
Boulder: Univ. of Colorado at Boulder;
Ithaca: Cornell Univ.;
College Station: Texas A&M Univ.;
Knoxville: Univ. of Tennessee;
Notre Dame: Univ. of Notre Dame;
Columbus: The Ohio State Univ.;
Minneapolis: Univ. of Minnesota;
Princeton: Princeton Univ.;
Rochester: Univ. of Rochester;
Mayaguez: Univ. of Puerto Rico;
West Lafayette: Purdue Univ.;
Hammond: Purdue Univ.
Lincoln: Univ. of Nebraska-Lincoln;
Cambridge: Massachusetts Inst. of Tech.;
Melbourne: Florida Inst. of Tech.;
Gainesville: Univ. of Florida;
Iowa City: The Univ. of Iowa;
Baltimore: Johns Hopkins Univ.;
Buffalo: State Univ. of New York;
Manhattan: Kansas State Univ.;
Lawrence: The Univ. of Kansas;
Livermore: Lawrence Livermore National Lab.;
College Park: Univ. of Maryland;
University: Univ. of Mississippi;
Houston: Rice Univ.;
Evanston: Northwestern Univ.;
Hammond: Purdue Univ. Calumet;
New York: The Rockefeller Univ.;
Piscataway: Rutgers Univ.;
Charlottesville: Univ. of Virginia;

UZBEKISTAN
Tashkent: Inst. of Nuclear Phys. of the Uzbekistan Acad. of Sciences